Zhang, Mingyang; Kujala, Pentti; Hirdaris, Spyros

A machine learning method for the evaluation of ship grounding risk in real operational conditions

Published in:
Reliability Engineering and System Safety

DOI:
10.1016/j.ress.2022.108697

Published: 01/10/2022

Document Version
Publisher's PDF, also known as Version of record

Please cite the original version:
Zhang, M., Kujala, P., & Hirdaris, S. (2022). A machine learning method for the evaluation of ship grounding risk in real operational conditions. *Reliability Engineering and System Safety*, *226*, Article 108697. https://doi.org/10.1016/j.ress.2022.108697

Reliability Engineering and System Safety 226 (2022) 108697

Contents lists available at ScienceDirect

Reliability Engineering and System Safety

journal homepage: www.elsevier.com/locate/ress

A machine learning method for the evaluation of ship grounding risk in real operational conditions

Mingyang Zhang, Pentti Kujala, Spyros Hirdaris *

Department of Mechanical Engineering, Marine Technology, Aalto University, Otakaari 4, 02150, Koneteknikka 1, Espoo, Finland

ARTICLE INFO

Keywords:
Ship safety
Grounding risk
Big data analytics
Machine learning
Gulf of Finland

ABSTRACT

Ship groundings may often lead to damages resulting in oil spills or ship flooding and subsequent capsizing. Risks can be estimated qualitatively through experts' judgment or quantitatively through the analysis of maritime traffic data. Yet, studies using big data remain limited. In this paper, we present a big data analytics method for the evaluation of grounding risk in real environmental conditions. The method makes use of big data streams from the Automatic Identification System (AIS), nowcast data, and the seafloor depth data from the General Bathymetric Chart of the Oceans (GEBCO). The evasive action of Ro-Pax passenger ships operating in shallow waters is idealized under various traffic patterns that link to side - or forward - grounding scenarios. Consequently, an Avoidance Behaviour-based Grounding Detection Model (ABGD-M) is introduced to identify potential grounding scenarios, and the grounding probabilistic risk is quantified at observation points along ship routes in various voyages. The method is applied on a Ro-Pax ship operating over 2.5 years ice-free period in the Gulf of Finland. Results indicate that grounding probabilistic risk estimation may be extremely diverse and depends on voyage routes, observation points, and operational conditions. It is concluded that the proposed method may assist with (1) better identification of critical grounding scenarios that are underestimated in existing accident databases; (2) improved understanding of grounding avoidance behaviours in real operational conditions; (3) the estimation of grounding probabilistic risk profile over the life cycle of fleet operations and (4) better evaluation of waterway complexity indices and ship operational vulnerability.

1. Introduction

In recent years the influence of the economies of scale led to increased ship sizes, traffic intensity, and associated risks [1–3]. Ships are sensitive to risks associated with navigation patterns pretraining to grounding accidents [4,5]. Potentially disastrous consequences may result in loss of life and environmental damage [6–8]. A statistical review of accident records in the Gulf of Finland (GoF) shows that grounding/stranding events dominate 41.2 % of the accident records from 1990 to 2017 (see Fig. 1). From 2014 to 2017, there have been 153 grounding / stranding events accounting for 24.8 % of the accidents in the Baltic Sea [9].

Research on ship grounding risk assessment focuses on (a) probabilistic risk analysis models, (b) grounding consequence evaluation models, and (c) grounding avoidance algorithms.

Probabilistic risk models help estimate the risk of grounding accidents on the basis of accident records and expert judgment. The probabilistic risk methods used in this type of analysis are statistical models [10–13]; Fault Tree (FT) analysis methods [14,15,69]; Bayesian Network (BN) methods [16–21]. These models are useful to evaluate grounding probabilistic risk from a macro perspective in a specific sea area. However, these approaches do not quantify the impact of varying hydro-meteorological conditions on ship motions and operational safety indicators. Instead, they assume that the conception of hydrometeorological risks depend on expert judgement s. Inevitably, simplified assumptions limit model feasibility. Therefore it is challenging for these models to provide a convincing justification for grounding risk mitigation measures for ongoing ships during real shipping operations.

Grounding consequence evaluation models combine ship structural dynamics, such as Fluid-Structure Interaction (FSI) analysis [22–24] and Finite Element Model (FEM) [25,26]. These models are extremely useful within the context of risk-based ship design [27,28]. Nevertheless, similarly to probabilistic risk analysis models, they may underestimate grounding risk as they do not account for real environmental conditions or traffic uncertainty.

Those models that are based on grounding avoidance algorithms make use of evolutionary theory [29,30]; A* algorithm [31,32]; Ant

* Corresponding author.
E-mail address: spyros.hirdaris@aalto.fi (S. Hirdaris).

https://doi.org/10.1016/j.ress.2022.108697
Received 7 March 2022; Received in revised form 13 June 2022; Accepted 25 June 2022
Available online 2 July 2022

Nomenclature

Variable	definition
ABGD-M	avoidance behaviour-based grounding detection model
AIS	automatic identification system
ARPA	automatic radar plotting aid
β_i	the angle between the point of shallow and heading
BN	Bayesian network
C	cluster
ε	threshold parameter of DP algorithm
CADCA	collision avoidance dynamic critical area
COG	course over ground
CSI	cubic spline interpolation
DEM	digital elevation model
DP	douglas-peucker
DTW	dynamic time warping
FEM	finite element model
FSI	fluid-structure interaction
FT	fault tree
GEBCO	general bathymetric chart of the oceans
GT	gross tonnage
IMO	international maritime organization
depth	the depth of the seafloor
K	the clustering number
k_{DC}	distance factor
k_{RR}	risk reducing factors
l_i	the horizontal distance between the AIS transponder and bow
LAT, lat_n	latitude
LON, lon_n	longitude
μ_1	the defined centre trajectory in K-means
MAIB	marine accident investigation branch
MMSI	maritime mobile service identitY
N	the maximum number of iterations
T	timestamp in UTC time
NOAA	national oceanic and atmospheric administration
P_C	grounding causation probability
P_G	geometrical grounding probability
P_{NT}	the annual frequency of ships misses a turn
p_j	a point of ship trajectory
θ_i	the course of the selected ship
ROTi	rate of turn
Safe_C	safety contours corresponding to ship draft and under keel clearance
SOG	speed over ground
ST	ship trajectory
T_{length}	the length of the ship trajectory
T_{se}	locations of the departure and destination ports of a ship trajectory
TIMESTAMP	timestamp for a data packet in UTC time
CL	the ship trajectories centreline
UKC	under keel clearance
V and T	speed, draft
λ	check frequency
Bearing, β	the bearing angle from ship to shallow waters
CT	the centreline of ship trajectories
Dis_F	the distance between the AIS transponder and the shallow waters
Dis_L	the minimum distance between ship lateral to the shallow water of voyage i
Dis_i	the minimum distance between ship toward the shallow water of voyage i
Distance	the minimum distance between the observation point
$F()$	the cumulative distribution function
Isobaths	the isobaths of seafloor
$N(\mu,\sigma)$	normal distribution with two key parameters
V	ship traveling speed
WP	the key waypoints
$d(p_j,p_{j+1})$	the distance between p_j and p_{j+1}
dis	the distance between missed turning point and the edge of the safety contour
$f()$	a complicated function on determining safety contours
∂	ship headings
$F()$	the cumulative distribution function (CDF)
Potential_ship	ship point during ship taking evasive action
Potential_location	locations of potential grounding on safety contour

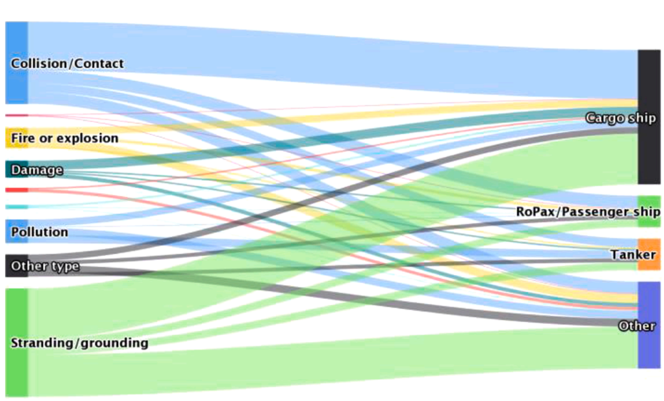

Fig. 1. Number and type of accidents in the Gulf of Finland (1990–2017).

Colony optimization methods [33,34]; Fast Marching schemes [35,36] or the CADCA (Collision Avoidance Dynamic Critical Area) approaches [37–39]. These algorithms may be useful to determine ship routes away from shallow water areas. However, they often underestimate ship manoeuvring in real operational conditions and are over-simplified as they do not account for real operational conditions. Research on understanding grounding avoidance behaviour of passenger ships using big data is very limited and concentrates on ship manoeuvring simulations [37,40] or the introduction of simplistic traffic management methods [41–44]. Lately, Montewka et al. [40] presented a method to quantify traffic complexity and grounding risk around own ship. However, their study did not account for the influence of hydro-meteorological conditions.

Advances in big data analytics and the emergence of machine learning could offer the opportunity to develop improved grounding risk management models and intelligent decision support systems based on the combination of experience, environmental, and traffic data records [1,45,46]. In this paper a multi-source integration model is used to integrate ship trajectories, hydro-meteorological conditions, and bathymetry data for the evaluation of grounding risk in real operational conditions. The K-means method [1,5] is used to cluster ship trajectories into various voyages. Dynamic Time Warping (DTW) [52,74] and Douglas-Peucker (DP) [2,54] methods are adopted to identify the key waypoints along the centre line of each of the clustered ship trajectories. Thus, the relationships between ship traffic behaviours and operational conditions under which the potential grounding scenarios may occur are investigated in various routes using machine learning. The timing for triggering grounding avoidance behaviors in various operational

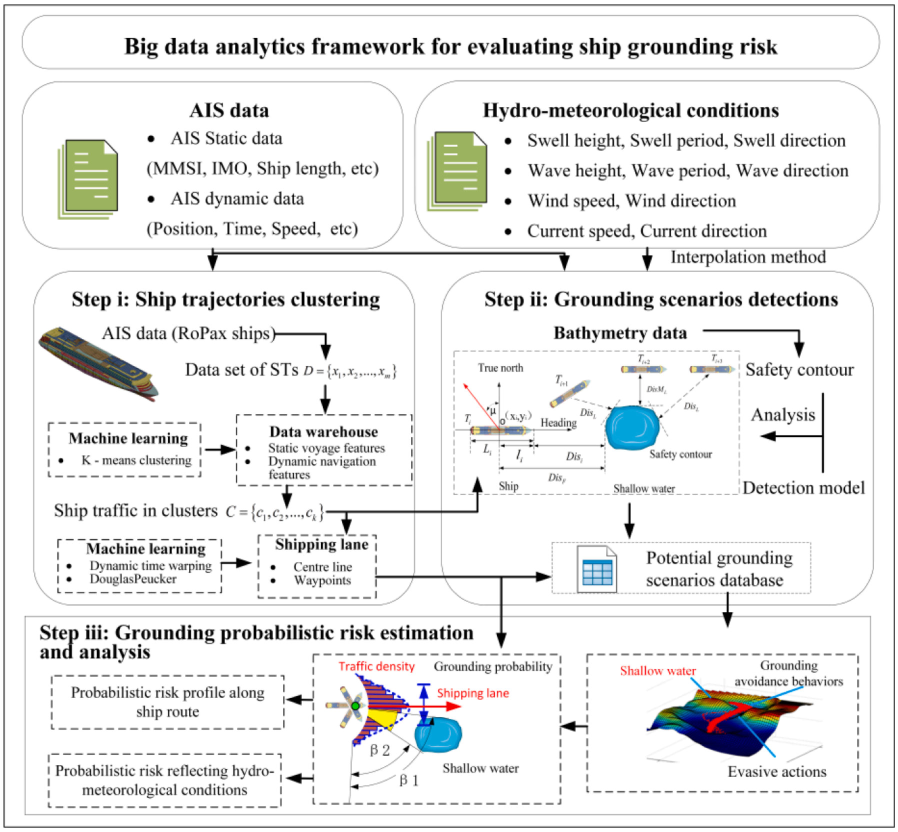

Fig. 2. The framework of grounding risk evaluation using big data analytics.

Table 1
Ship trajectories clustering method using K Means algorithm.

Algorithm 1: K-means algorithm for ship trajectories clustering
Input:
Dataset $D = \{x_1, x_2, ..., x_m\}$, clustering number K, the maximum number of iterations N
Output:
Clustering $C = \{c_1, c_2, ..., c_k\}$
Process:
1. Select K trajectories as the centre trajectories $\{\mu_1, \mu_2, ..., \mu_k\}$;
2. Initially cluster division $C_t = \{c_1, c_2, ..., c_k\}$;
3. For $n = 1, 2, ..., N$:
4. For $i = 1, 2, ..., m$:
5. Calculate distance between the trajectory x_i and $\mu_j (j = 1, 2, ..., k)$ $d_{ij} = |x_i - \mu_j|$;
6. Mark category as j corresponding the smallest d_{ij};
7. End for
8. For $j = 1, 2..., K$:
9. Calculate the centre trajectories based on the new clustering result
$$\mu^j = \frac{1}{|\mu^j|}\sum x(x \in \mu^j)$$
10. End for
11. If the clustering result remains consistent:
12. Go to line 17;
13. Else:
14. Go to line 4;
15. End if
16. End for
17. Output $C = \{c_1, c_2, ..., c_k\}$.

conditions is further analyzed to provide support information for grounding avoidance. The proposed approach is introduced in Section 2. Results and analysis based on ship operations over a 2.5 year ice-free period (2017-2019) in the Gulf of Finland are demonstrated in Section 3. Conclusions on the potential application of intelligent decision support systems grounding risk mitigation for ongoing ships in real operational conditions are presented in Section 4.

2. Big data analytics framework for the evaluation of ship grounding risk

The high-level framework for the evaluation of ship grounding risk in real operational conditions is shown in Fig. 2. The framework aims to illustrate the trends, patterns, and correlations of grounding risk in real operational conditions by utilising big data streams. Accordingly, decision support safety criteria (safety indicators) can be provided to the master. Three key steps of the grounding risk evaluation framework are outlined:

- In **step (i)** ship trajectories (STs) are reconstructed and clustered using AIS data. Then, the key waypoints along the centre line of each cluster are determined using DTW and DP algorithms.
- **Step (ii)** focuses on the detection of ship grounding scenarios. For each cluster identified under step (i), Under Keel Clearance (UKC) information and ship draft are used to determine bathymetry isobaths and define safety contours in shallow waters. Consequently, forward and side grounding scenarios are identified using a proposed avoidance behavior-based grounding detection model. The grounding scenarios and associated with those hydro-meteorological data are stored in a database [5].
- **Step (iii)** evaluates the probabilistic risk of ship grounding. For each of the scenarios shortlisted under step (ii), the risks are evaluated at various observation points along the ship route and probabilistic risk profiles are analysed in various hydro-meteorological conditions.

Further details associated with each of these steps are outlined in the following sections.

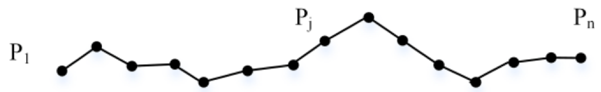

Fig. 3. Defined ship trajectory using AIS data.

Table 2
DTW algorithm for the extraction of ship trajectory centreline.

Algorithm 2: Ship trajectories centreline extraction
Inputs: $STs = \{ST_1, ST_2, ST_3, \cdots, ST_N\}$
Outputs: Ship trajectory centreline CT
Process:
1: Let original centreline $CT_1 = ST_1$
2: For each ship trajectory ST $_i$ in route do
3: Let ST $_i$ align to centre path $CT_i = DTW(CT, ST_i)$
4: For each point p_l^{γ} in CT_{γ} do
5: $CT_i = \dfrac{p_l^{\gamma} \times i + ST_i}{i+1}$
6: End For
7: End For
8: Return $CT$of STs

2.1. Step (i): ship trajectories clustering and key waypoints determination

This step focuses on voyage classification and key waypoints extraction using AIS data. At first, ship trajectories corresponding to different voyages are separated. Following data filtering (i.e., error detection and removal of outliers) [47–49], data are interpolated [50, 51] and then clustered into various groups [1,5]. The sub-steps of the process are defined as follows:

(1) At first instance, to avoid collection, transmission, and reception errors, wrong timestamps or irrational speeds/locations contained in AIS data are thoroughly reviewed. Consequently, static data (e.g., ship length, ship width, etc.) are updated in the MMSI format.
(2) AIS data records are reconstructed on the basis of interpolation over 60 s intervals [1,51].
(3) Ship trajectories representing different routes are clustered by the K-means method (see in Table 1). This approach accounts for static - (e.g., departure / destination ports, length of ship trajectories, etc.) and dynamic - navigation features (e.g., course, heading, etc.) [1,71].

The mathematical background to this process is displayed in Eqs. (1)–(4) below and the pseudocode of the process is summarised in Table 1. For a point p_i in the way of a trajectory defined as per Eq. (1), the locations of the departure and destination ports are defined as in Eq. (2). Then the length of the ship trajectory is calculated as in Eqs. (3) and (4).

$$p_i = \{MMSI, TIMESTAMP, LON, LAT, SOG, COG,\ Draft\} \tag{1}$$

$$T_{se} = \{(lon_1, lat_1), (lon_n, lat_n)\} \tag{2}$$

$$d(p_j, p_{j+1}) = (TimeStamp_{j+1} - TimeStamp_j) \times \frac{sog_j + sog_{j+1}}{2} \tag{3}$$

$$T_{length} = \sum_{j=1}^{n-1} d(p_j, p_{j+1}) \tag{4}$$

where (lon_1, lat_1) and (lon_n, lat_n) denote the longitude and latitude of the departure and destination ports, respectively. $d(p_j, p_{j+1})$ denote the distance between p_j and p_{j+1} (see Fig. 3).

The ship trajectory centreline of each cluster is extracted using the Dynamic Time Warping (DTW) method introduced by Zhang et al. [52]. This is a classical distance measurement method to find an optimal

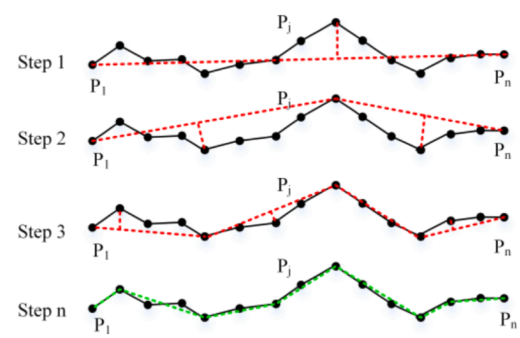

Fig. 5. The steps of the DP algorithm (The black line represents the original ship trajectories centreline, and the red line represents the simplified ship trajectories centreline. The idea of the simplified ship trajectories centreline is to approximate the original trajectory in green.).

Table 3
DP algorithm for the extraction of key waypoints.

Algorithm 3: Douglas-Peucker Algorithm
Inputs:
Require: CL (Points); ε (thresholds)
Parameter d (distance), dm (maximum distance), index
Outputs:
Waypoints $WP = \{p_1, p_2, ..., p_k\}$
Process:
1: For i = 2 to i=(n-1)
2: d = VD ($CL[i]$, $Line[CL[1], CL[n]]$)
3: If d > dm
4: index = i
5: dm = d
6: End if
7: End if
8: If dm >= ϵ
9: WaypointLList = DP (CL[1……index], ε)
10: WaypointRList = DP (CL[index……n], ε)
11: Waypoints= {WaypointLList, WaypointRList}
12: Else
13: Waypoints = {CL[1], CL[n]}
14: End if
15: Return Waypoints

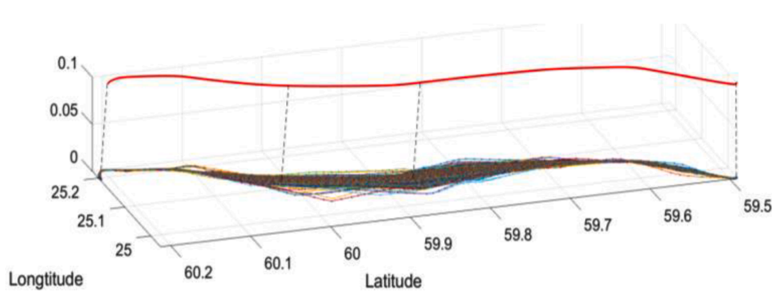

Fig. 4. An example of ship trajectories centreline in real operational conditions.

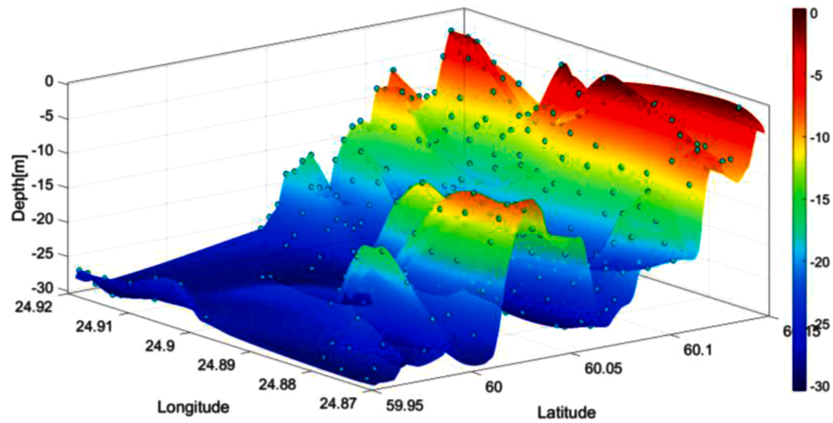

Fig. 6. Formation with seabed using bathymetry data (The point denotes the spatial data of GEBCO. The surface shows the bathymetry map of the seabed.).

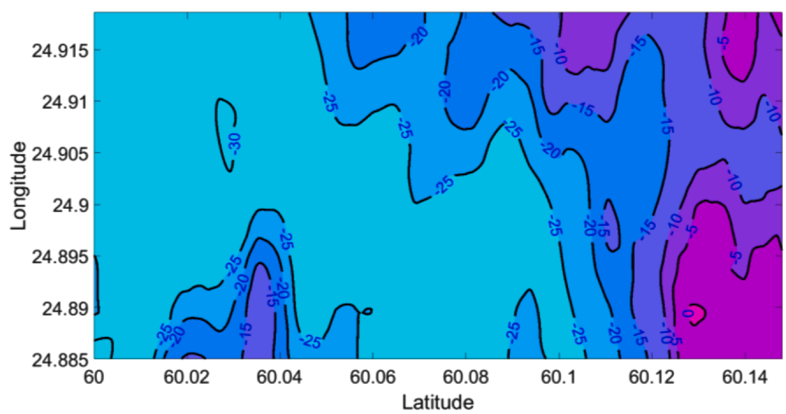

Fig. 7. The determined isobaths are based on bathymetry data, considering the safe water depth of the ship.

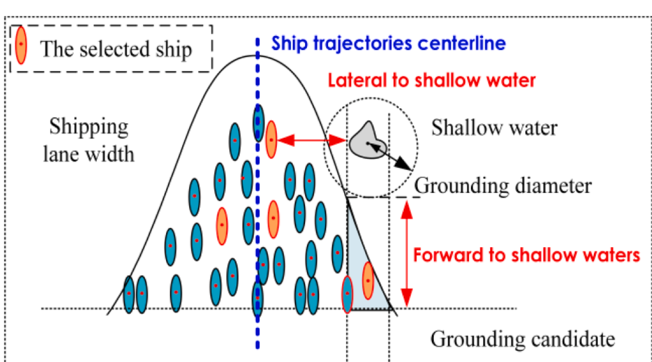

Fig. 8. The minimum distance for anti-grounding between ships and shallow waters.

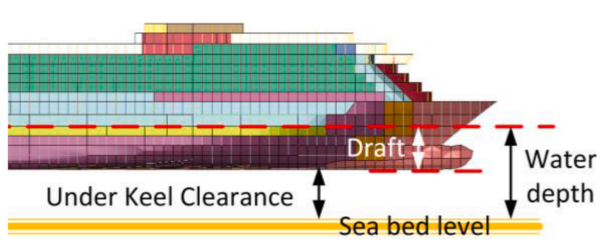

Fig. 9. Relationship between water depth, ship draft, and UKC.

alignment between two-time varying sequences under certain restrictions (see Table 2 and Fig. 4). The centreline of ship traffic can be determined to represent the ship trajectories for the extraction of key waypoints. The DP algorithm is used to determine the key waypoints of the ship route. These key waypoints can be used to represent the geographical locations where the ship takes evasive action by changing course [53–56]. Fig. 5 and Table 3 show the steps of the DP algorithm. Step 1 can be used to generate an approximated line segment between the departure and destination points. Steps (2, 3, …,n) introduce sub-line segments using various threshold parameters ε (see Section 3).

2.2. Step (ii): Detection of ship grounding scenarios

In this step the Avoidance Behaviour-based Grounding Detection Model (ABGD-M) introduced by Zhang et al. [5] is used to identify potential grounding scenarios in real hydro-meteorological conditions. The forward - and side - grounding scenarios are detected by making use of big data streams from AIS, nowcast data, and GEBCO.

2.2.1. Bathymetry data analysis for safety contours extraction

This part of the analysis makes use of GEBCO (2019) bathymetry data sets (see Figs. 6 and 7). Spatial data are interpolated by a generic mapping tool [57]. A Digital Elevation Model (DEM) [58] and a contour function are used to determine isobaths and define safety contours in the way of shallow waters (see Fig. 7). The defined safety contours reflecting draft and UKC are determined by isobaths; see Eq. (5). Safety contours corresponding to ship draft and UKC are defined according to Eq. (6).

$$Isobaths = f(lon, lat, depth) \tag{5}$$

$$Safe\_C = f(lon, lat, -(\text{draft} + UKC)) \tag{6}$$

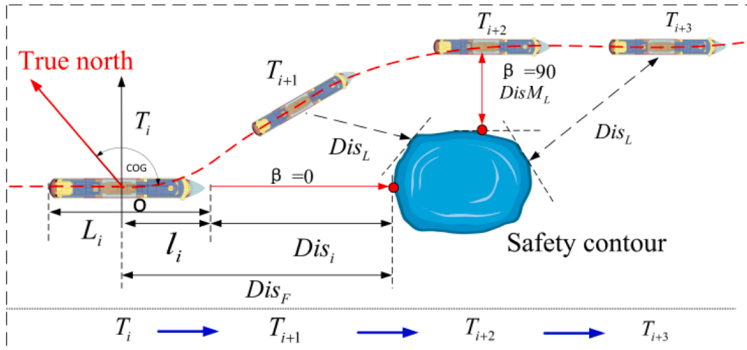

Fig. 10. The relationship between the shallow water and the spatial AIS data of a selected ship (Red dot line denotes ship trajectory, and red scatters denote the potential geographical locations of ship forward/side grounding.).

Table 4
The pseudocode for potential grounding scenarios detections.

Algorithm 4: Potential grounding scenarios detections
Input:
Dataset $C = \{c_1, c_2, ..., c_k\}$, $c_i = \{\mu_1, \mu_2, ..., \mu_n\}$, $\mu_i = \{p_1, p_2, ..., p_m\}$, ship trajectories clusters number K; the maximum number n of voyages in each cluster; the maximum number of points $m$of the ship trajectories μ_i.
Output:
Side grounding avoidance action $Dis_L = \{Dis_{L1}, Dis_{L2}, ..., Dis_{Ln}\}$
Forward grounding avoidance action $Dis_F = \{Dis_{F1}, Dis_{F2}, ..., Dis_{Fn}\}$
Process:
1. Determine the safety contour near to shallow water $\{S_1, S_2, ..., S_t\}$
2. Select the first cluster from$C = \{c_1, c_2, ..., c_k\}$;
3. For $K = 1, 2, ..., k$;
4. For $i = 1, 2, ..., n$;
5. For $q = 1, 2, ..., t$;
6. Calculate distance between ship point p_i and $\mu_j (j = 1, 2, ..., m)$ d_{mt}within 6 nm;
Select ship trajectory point p_i, if the bearing angle is between [355,0] and (0,5], and saved as Df_n;
Select ship trajectory point p_i, if the bearing angle is between [85,95] or (265,275], and saved as Dl_n;
7. Calculate minimum distance for anti-grounding $Dis_L = Min.(Dl_n)$ and $Dis_F = Min.(Df_n) - l_i$ While bearing angles Δβ is maximum.
8. End for
9. For $q = 1, 2, ..., t$:
10. End for
11 For $i = 1, 2, ..., n$:
12. End for
13. For $j = 1, 2..., K$:
14. Output $Dis_L = \{Dis_{L1}, Dis_{L2}, ..., Dis_{Ln}\}$;$Dis_F = \{Dis_{F1}, Dis_{F2}, ..., Dis_{Fn}\}$

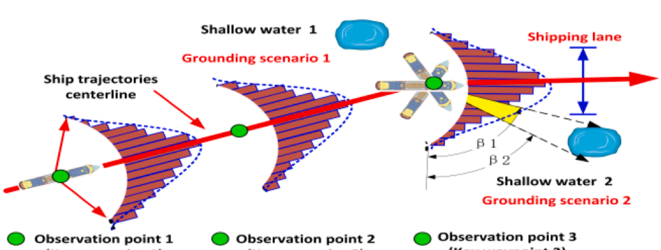

Fig. 11. A probabilistic risk model for the estimation of ship grounding along a selected route (At observation point 2, the ships may underestimate evasive actions due to a missed turn or late turn, leading to forward grounding on shallow water 1; At observation point 2, side grounding accidents may occur on shallow water 2 due to imprecise navigation resulting from the human factor, external conditions, etc.).

In the above equations $f()$ represents a complicated function that determines which isobaths (sea depth) each position (longitude-latitude pair) corresponds with.

2.2.2. Detection of grounding scenarios in real operational conditions

In this step AIS and GEBCO data are combined to idealize forward - and side - grounding scenarios that may be in general attributed to adverse environmental conditions, crew negligence, or technical failure (see Fig. 8). For example, forward - grounding may be linked to the case of a ship missing a turn. So, the potential forward grounding scenarios are detected where the ship takes evasive actions. On the other hand, side - grounding may relate to the case of a ship navigating under adverse environmental conditions too close or along shallow waters. Such grounding models consider terms such as vessel acceleration, bearing angle from ship to shallow waters and heading, rate of turn, dynamic draft, vessel course, etc., that may be used to identify the minimum distance for grounding avoidance (see Fig. 8).

Ship grounding scenarios are detected in the following three sub-steps:

- At first, safety contours are determined in the way of shallow waters by bathymetry data charts. Safe water depths or safety contours for the operation of the selected ship are based on draft and UKC corresponding to each voyage (see Fig. 9). It is noted that (10% × draft) is considered adequate for ships operating at port. However for navigation in waterways (20% × draft) is considered essential ([75, 76]). Accordingly, in this paper safety contours are defined according to Depth=-(draft + UKC) for UKC=20% × draft [59]. Consequently, the safety contour can be extracted from the factor of the ship to safety contour - *Safe_C* defined in Eq. (6).
- At second stage ship traffic data from shallow water observations within the 6 nautical miles conventional radar range are collected [1, 60–62] and the ship coordinate system is converted in relation to the direction and positioning of the grounding target (see Fig. 10). The bearing angles and distances are calculated from ship to safety contour *Safe_C* along different ship trajectories as shown in Fig. 10. The minimum distances for ship grounding evasion in real conditions are identified to determine the waypoints where ships usually make a turn. For side grounding scenarios, the minimum distance is calculated while the bearing angles are located into the interval [85, 95] or [265, 275], as shown in Eqs. (7) and (8). After this point, the ship moves away from shallow waters. Thus, the critical points are defined as the time of evasive action taken to avoid side grounding.

$$Dis_L(Tr_i, Safe\_C_j) = Dist(lon_n^i, lat_n^i, lon_m^j, lat_m^j | Bearing),\ Bearing \in [85, 95] \cap [265, 275] \tag{7}$$

$$DisM_L^i = Min.[Dis_L(Tr_i, Safe\_C_j)] \tag{8}$$

For forward grounding scenarios, the minimum distance is calculated based on Eqs. (9) and (10), while the bearing angles are located

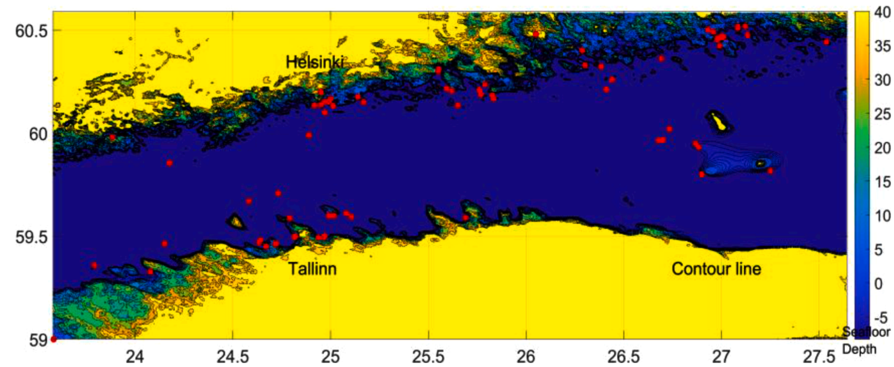

Fig. 12. Positions of the groundings in the Gulf of Finland between the years 1997 and 2017 (Red scatters represent the location of grounding accidents. There have been 10 grounding / stranding events accounting for Ro-Pax ships).

Table 5
Bathymetry data fields available for the presented model

Data field	Unit	Description
Position	-	Latitude and longitude
Depth value	m	Delivered from GEBCO database
Source identifier grid	-	The way of depth value collected

into the interval $(355, 360)$ or $(0, 5)$. To further analyse grounding avoidance behaviours, the critical point associated with the maximum rate of bearing angles $\Delta\beta$ before the point with minimum distance is determined and defined as the time of evasive action taken to avoid forward grounding.

$$Dis_F(Tr_i, Safe\_C_j) = Dist(lon_n^i, lat_n^i, lon_m^j, lat_m^j | \text{Bearing}),\ \text{Bearing} \in [355, 360] \cap [0, 5] \tag{9}$$

$$Dis_i = Min.[Dis_F(Tr_i, Safe\_C_j)] - l_i \tag{10}$$

- In the final stage bathymetry data are cross-checked for water depths below the originally safe water depths and isobaths are calculated (see Fig. 7). For various voyages, the extracted *Safe_C* is different due to the dynamic ship draft. Thus, the process of grounding scenario detection is carried out of each ship trajectory. For example, as shown in Fig. 10, a ship sails on the red track, encountering shallow water based on her dynamic draft. At T_i, the ship is ahead of shallow waters and the rate of bearing angle $\Delta\beta$ is at its maximum, showing that the ship starts to change course for grounding risk mitigation. In this case the forward grounding event will occur if the ship does not take any grounding evasive actions in time. At T_{i+1}, the bearing angle is out of the interval $(355, 360)$ or $(0, 5)$. This indicates that the evasive action works to avoid forward grounding and coming to the next stage. At T_{i+2}, the bearing angle is located into the interval $(85, 95)$, and the distance from ship to shallow water is minimum. Side grounding may occur due to imprecise navigation resulting from adverse hydro-meteoritical conditions, etc. At T_{i+3}, the bearing angle is out the interval $(85, 95)$, and the ship is away from the shallow water. Consequently, the mentioned critical points of ship trajectory at T_i and T_{i+2} and corresponding geographical locations on safety contour are stored as shown in Eqs. (11) and (12) for grounding behaviour analysis.

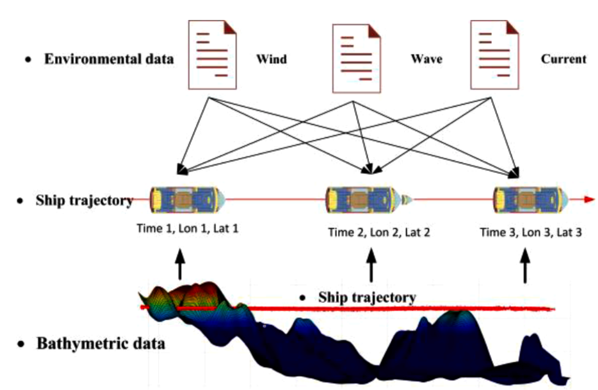

Fig. 14. Big data integration of AIS, bathymetry data, and hydro-meteorological data for grounding risk evaluation.

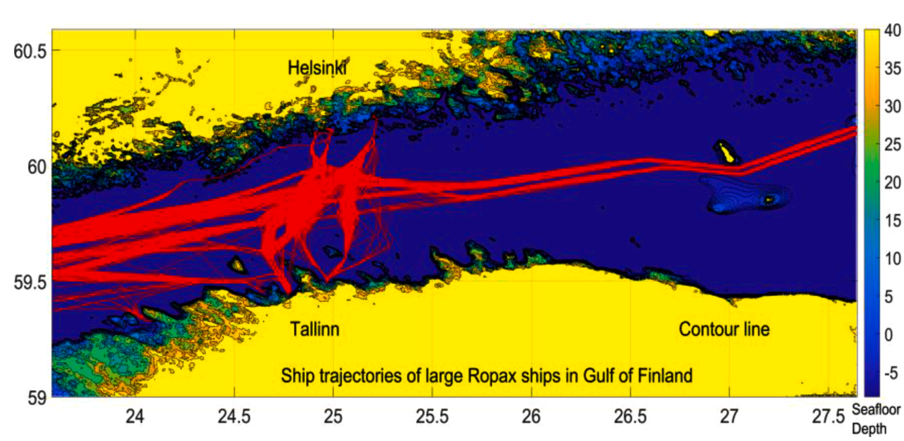

Fig. 13. Ship trajectories mapping on bathymetry map.

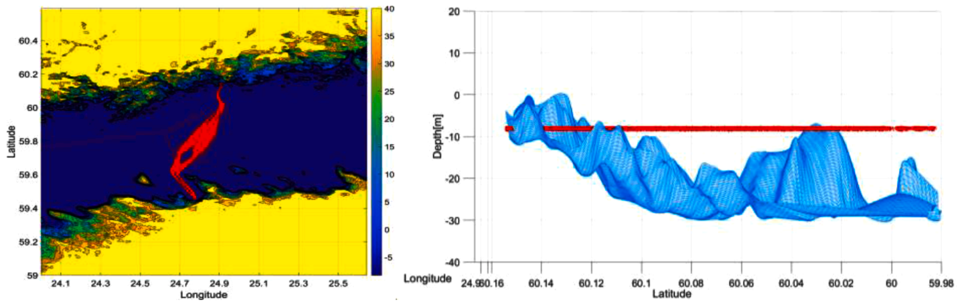

Fig. 15. The seabed level with the recorded denoised ship trajectories of the selected ship delivered from AIS data (top and side view).

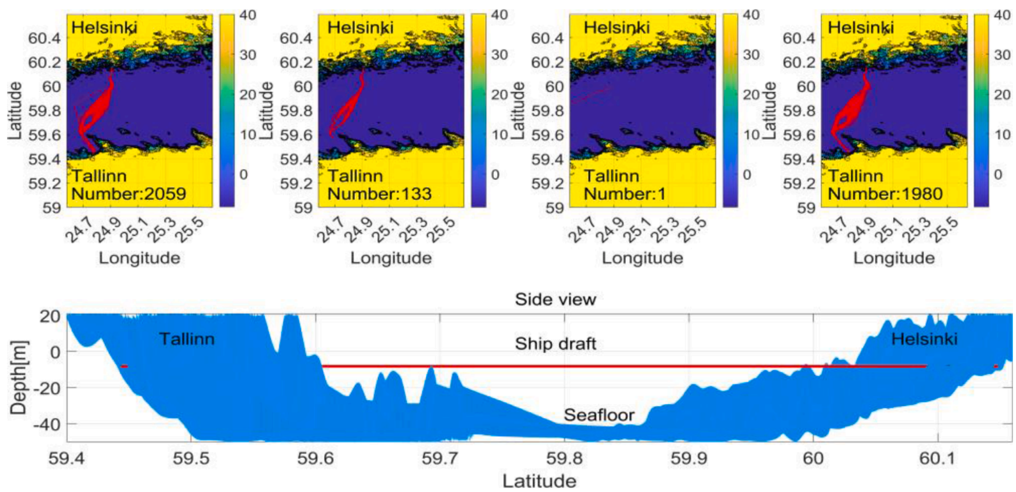

Fig. 16. The selected ship trajectories of clustered results on the bathymetry map.

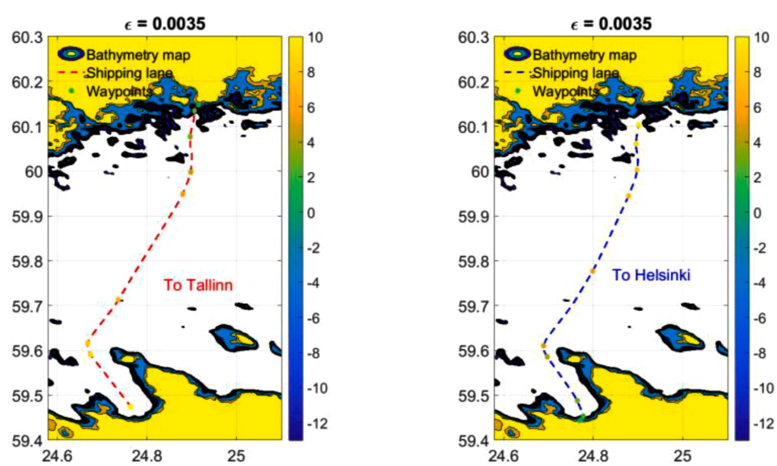

Fig. 17. The determined ship navigation lanes between Helsinki and Tallinn using DTW.

$$Potential\_ship = Tr(dynamic\_data, static\_data)|potential\_Scenarios) \quad (11)$$

$$Potential\_location = f(lon, lat, -(draft + UKC)|potential\_Scenarios) \quad (12)$$

The overall avoidance mechanism of grounding behaviour is analysed by AIS, GEBCO, speed, and bearing angles suitable for the identification of the forward and side grounding scenarios using the pseudocode shown in Table 4.

2.3. Step (iii): Estimation of the probability of ship grounding

The estimation of the probability of ship grounding is meaningful before and after a ship takes evasive actions. In this paper, the well-established approach proposed by COWI (2008) [63] was adopted to evaluate ship traffic distributions for grounding risk assessment at various observation points (key waypoints) determined in Step (i) in real operational conditions (see in Fig. 11).

Side grounding accidents often occur due to imprecise navigation

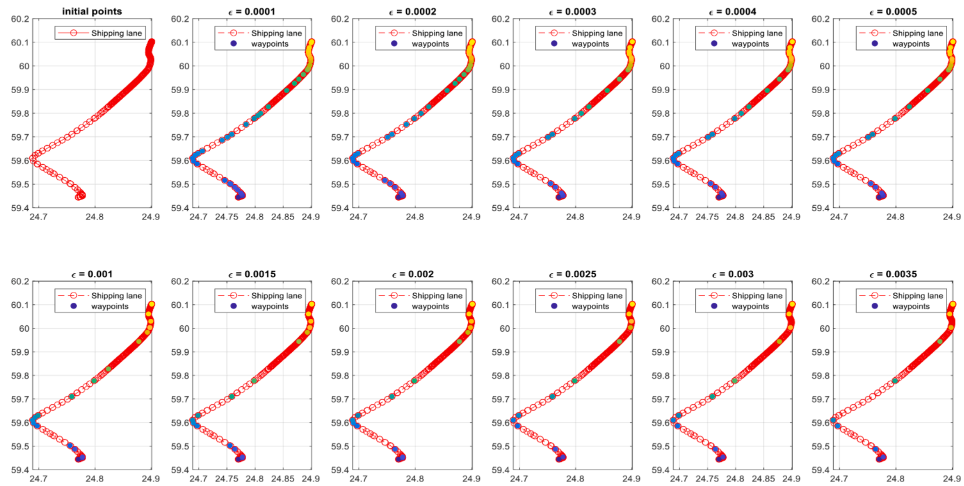

Fig. 18. Key waypoints determination using DP algorithm with the various threshold parameters.

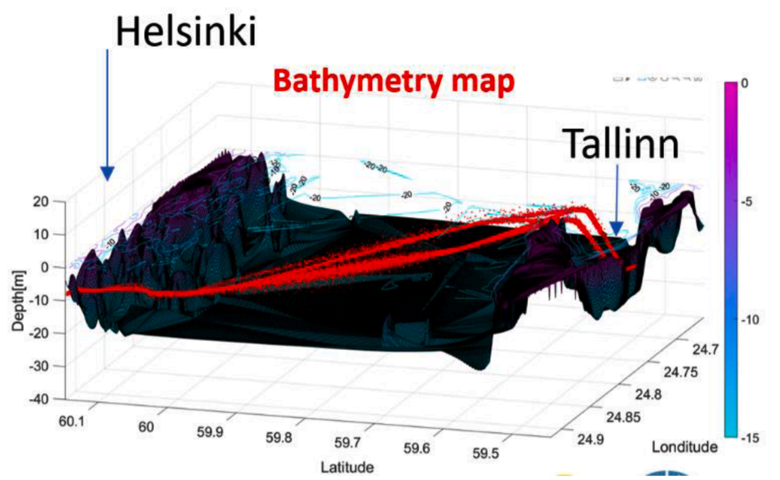

Fig. 19. The seabed level with the recorded ship trajectories delivered from AIS data (The red continuous line outlines the ship trajectories between Helsinki and Tallin).

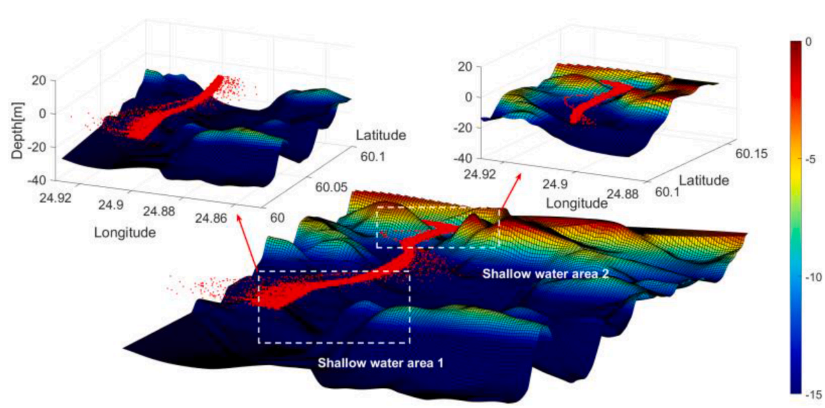

Fig. 20. The relationship between isobaths and ship trajectories near shallow waters.

resulting from adverse hydro-meteorological conditions, crew negligence, technical failure, etc. This grounding type often occurs in various water areas when the route channel is complex and the crews onboard are not aware the ship is navigating toward shallow waters [5,64]. This may result in the underestimation of evasive actions in real operational conditions. The geometrical grounding model is established by evaluating the ship travel behaviors a few nautical miles before they pass shallow water. The geometrical probability of this type of grounding can be evaluated based on the bearing angle distributions as:

$$P_G = F(\beta_1) - F(\beta_2) \tag{13}$$

A Normal distribution $N(\mu, \sigma)$, Log-normal distribution $Ln(\mu_1, {\sigma_1}^2)$ or

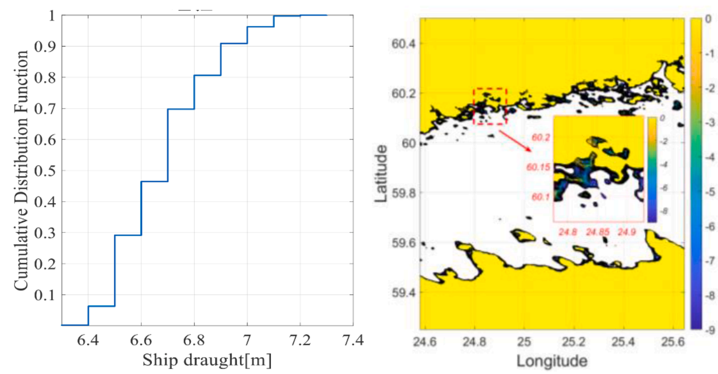

(a) Draft cumulative distributions (b) Safety contours corresponding to dynamic draft

Fig. 21. Draft cumulative distributions and the corresponding safety contours for the selected ship.

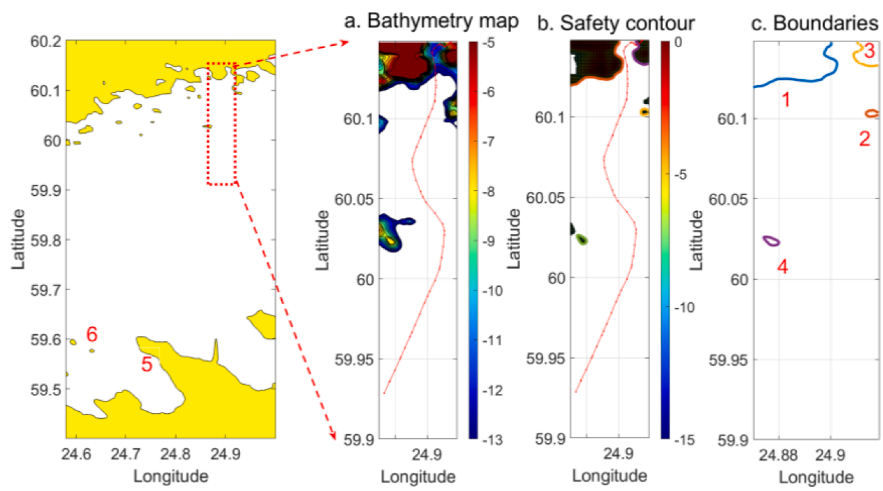

Fig. 22. The ship trajectory and the corresponding safety contours (the red line denotes a ship trajectory from Tallinn to Helsinki.).

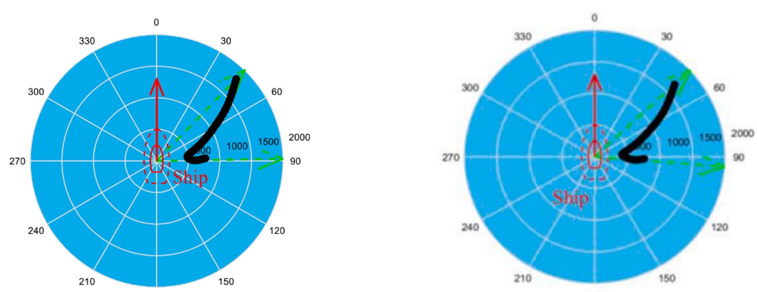

(a)Observation point 1 (timestamp: 1489129878) (b) Observation point 2 (timestamp: 1489129938)

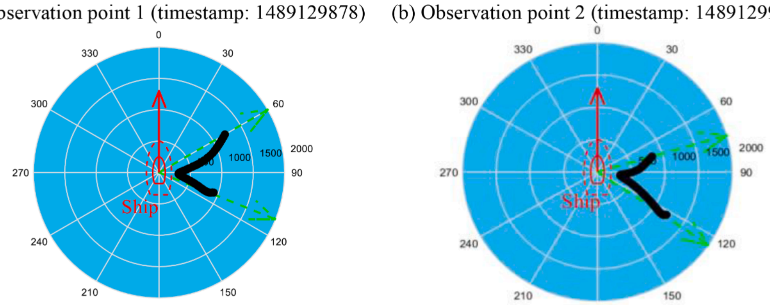

(c) Observation point 3 (timestamp: 1489129998) (d) Observation point 4 (timestamp: 1489130004)

Fig. 23. The coordinate system of ship and safety contour from own ship perspective (The black line denotes the yellow safety contour 3 in Fig. 22(c).).

Table 6
Summary of the shallow water areas and detected potential grounding hotspots.

Shallow waters	Grounding type	Helsinki to Tallinn	Tallinn to Helsinki
6	Forward grounding	4 hotspot areas*	6 hotspot areas
	Side grounding	6 hotspot areas	6 hotspot areas

*For shallow waters 1 and 3 in Fig. 22, we did not detect any forward grounding from Helsinki to Tallinn.

combination is usually fitted to present the bearing angles from ship to shallow waters (see in Fig. 11). Consequently, the parameters of the best-fitted distributions are calibrated at each observation point. $F()$ denote the cumulative distribution function (CDF) of bearing angle with regard to clockwise angle β. And β_1 and β_2 are critical bearing angles in the ship heading towards the grounding location indicated in Fig. 11. The annual grounding frequency of scenarios at an observation point x is presented as:

$$P_x = NP_G P_C k_{DC} k_{RR} \tag{14}$$

$$P_R = \sum_{x=1} (P_x), x = 1, 2, 3, 4, \cdots \tag{15}$$

where N denotes the number of ships passing the route covering one year period, P_C denotes the causation probability that ships do not take grounding avoidance behaviors; k_{RR} denotes risk-reducing factors (i.e., pilotage effect, operational instructions, and procedures by the shipping company), which often is defined 0.5 (COWI 2008); k_{DC} denotes distance factor presented as

$$k_{DC} = \frac{x}{distance} \tag{16}$$

where *distance* denotes the minimum distance between the observation point and the boundary of the safety contour; x is defined as 10 nm [63, 64].

A forward grounding scenario relates to a missed turn or late turn of a ship in shallow waters. The frequency of the forward grounding scenario is calculated as:

$$P_X = NP_{NT} P_G P_C k_{RR} \tag{17}$$

where P_G is geometrical grounding probability computed in Eq. (13). P_{NT} is the annual frequency of ships missing a turn. According to COWI (2008) [63], a missed turn frequency is defined as:

$$P_{NT} = e^{-\lambda \frac{dis}{V}} \tag{18}$$

where λ is the check or observation frequency of crew (0.5–1 min) [64]; *dis* is the distance between missed turning point and the boundary of safety contour; V is ship traveling speed.

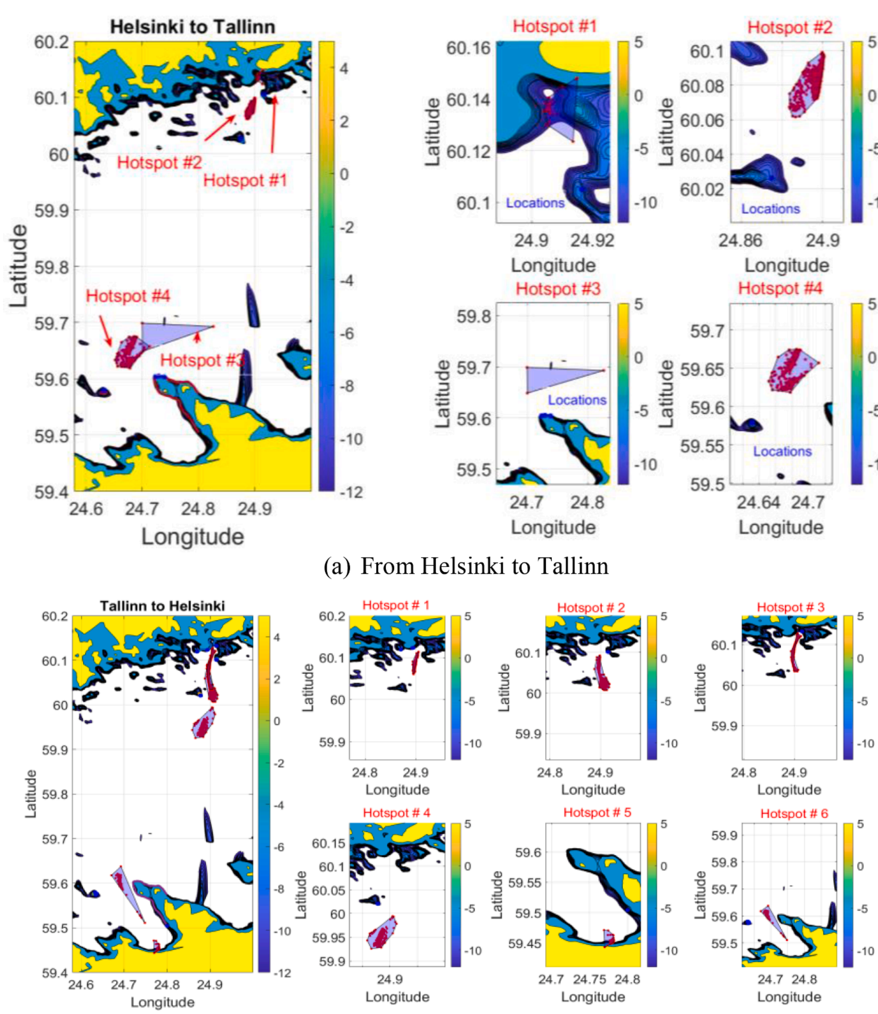

(a) From Helsinki to Tallinn

(b) From Tallinn to Helsinki

Fig. 24. Identification of potential forward grounding scenarios (The geographical locations of possible grounding points were identified as shown by the blue points on safety contours. Red points denote locations of grounding avoidance.).

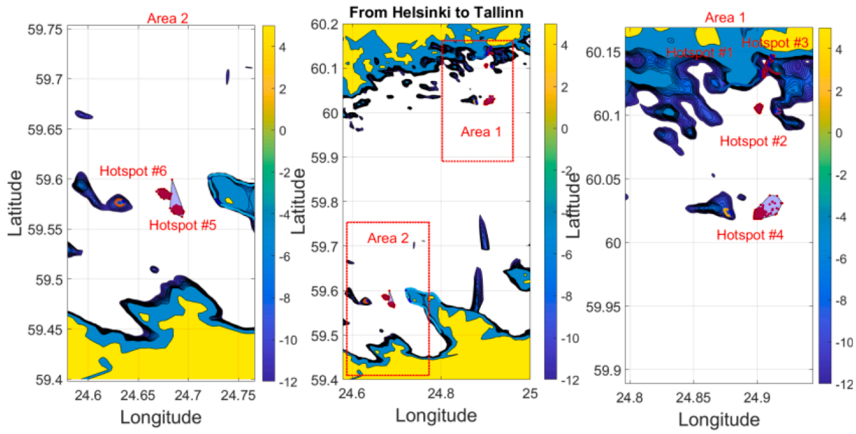

(a) From Helsinki to Tallinn

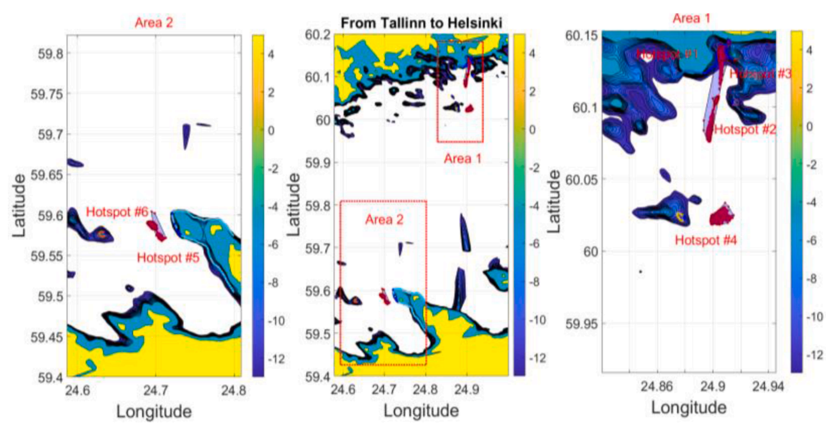

(b) From Tallinn to Helsinki

Fig. 25. Identification of potential side grounding scenarios. (The geographical locations of possible grounding points were identified as shown by the blue points on safety contours. Red points denote locations of grounding avoidance.).

3. Case study

Variable bathymetry in mild or extreme environmental conditions may result in grounding accidents (see Fig. 12). A case study is carried out by using AIS data, bathymetry data and environment data in the Gulf of Finland. The Gulf of Finland may be ice-covered in December, January, February. Thus, the ice-free period between 2017 and 2019 is considered here as dominating in the paper.

3.1. Data sources and integration

The case study presented in this paper makes use of available AIS big data records from *VesselTracker, FleetMon*, and *MarineTraffic* for a typical Ro-Pax ship cruising between 2017 and 2019 during ice-free period. And the sea bottom was mapped using GEBCO (2019) data (see Table 5 and Fig. 13). Shallow waters were determined in the vicinity of ship operational areas using available bathymetry, draft, and UKC information. Now-cast hydro-meteorological data, covering the study area, are downloaded from the records made available by the providers [1].

Following the review of historic AIS, and bathymetry records data and environmental data were interpolated and integrated into ship trajectories for the evaluation of grounding risk (see Fig. 14). As a result, Fig. 15 presents the varying bathymetry and shallow waters, which may result in grounding accidents in the study area.

3.2. Results and analysis

3.2.1. Ship voyage classification and key waypoints extraction

Ship trajectories for the selected vessel were extracted from the AIS database and then separated based on the distribution of time intervals for each voyage [73,74]. The vector format of ship motion parameters (e.g., ship speed, course, bearing angle to shallow waters, etc.) were updated every 6 min using Radar and ARPA records [3,38]. The frequency of AIS transmission depends on ship behavior and at port, the frequency of AIS transmission is higher than 6 min [67,70]. To address this point 360 s time intervals between two ship points (defined as start and end of the voyage) were set as a threshold, and ship trajectories were separated into various voyages [51,52]. After separating ship trajectories and deleting white noises or errors, ship trajectories were reconstructed using AIS data records interpolated over 60 s intervals [1,52].

For each ship trajectory, the dynamic and static data were used to cluster ship trajectories as explained in Section 2.1 (Fig. 3 and Table 1). The process concluded on two main clusters, namely: (a) Cluster 1 containing 2,059 complete voyages from Helsinki to Tallinn; (b) Cluster 2 containing 1,980 complete voyages from Tallinn to Helsinki (see Fig. 16). The side view of ship trajectories and bathymetry map shown in Fig. 16 demonstrates that waterway traffic nearby Helsinki and Tallinn ports is complex and bathymetry restricts ship operations.

For each main cluster, the ship navigation lanes (ship trajectories

[1] Now-cast hydrometeorological data were accessed from the following data bases (i) USA National Oceanographic and Atmospheric Administration (https://www.noaa.gov/) for wind speed and direction; (ii) Tidetech (https://www.tidetech.org/) for wave height, period, tidal currents and water levels; (iii) Mercator Ocean (https://www.mercator-ocean.fr) for ocean currents.

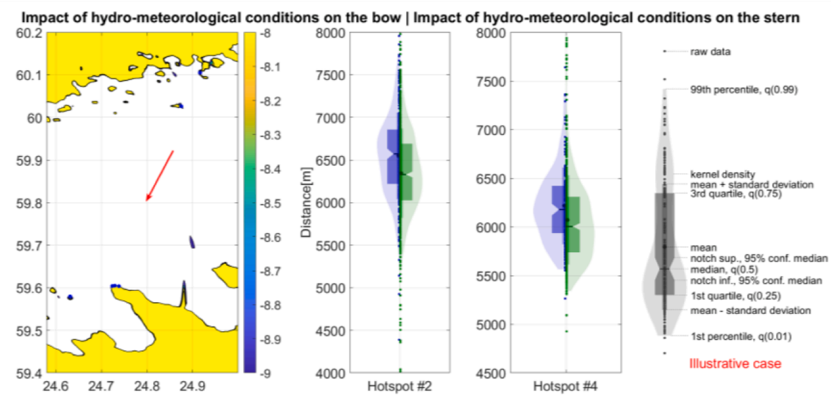

(a) Helsinki to Tallinn route

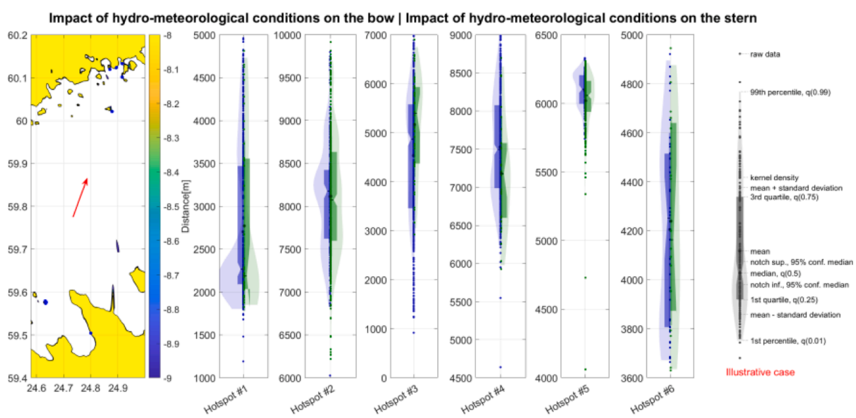

(b) Tallinn to Helsinki route

Fig. 26. Safety distance to shallow waters of the forward grounding scenarios in various hydro-meteorological conditions (The blue points on the bathymetry map denote the geographical locations of possible forward grounding scenarios if the evasive action was underestimated.).

centreline) were extracted using DTW and the key waypoints of ship navigation lanes were determined using the DP algorithm (see Section 2.1, Fig. 4 and Tables 2 and 3 for the theoretical concept and Fig. 17 for the application of the method). As part of this process sub-line segments were extracted using the DP algorithm with $\varepsilon = 0.35$ (see Fig. 18) [56].

3.2.2. Detection of grounding scenarios

The ship safety contours were extracted based on the dynamic ship draft and UKC. Fig. 19 outlines a sample seabed level map.

The observation distance of 6 nm radar radius was set to draw safety contours in way of shallow waters [16,40]. The depths of safety contours were determined based on the ship dynamic draft (see Figs. 20 and 21) and UKC = 20% $\times$ draft (see Scully and Young [75]; Orseau et al. [76]; Verwilligen et al. [59]). The cumulative distributions of ship drift T over the 2.5 years of operations are shown in Fig. 21.

GEBCO (2019) and AIS data were used to identify shallow water encounters (see Fig. 22). The isobaths boundaries of safety contours were determined according to Eqs. (5), (6) and (19). For the route between Helsinki and Tallinn, 6 shallow water areas were observed within 6 nm around the complex waterway (see in Fig. 22). Results were based on the following draft cumulative distributions:

$$Isobaths_{boundary} = (Isobath_1, Isobath_2, \cdots Isobath_t), t = 1, 2, 3, 4, \cdots \quad (19)$$

As shown in Section 2.2, to analyze grounding avoidance behaviours and the potential grounding locations, the ship coordinate system was converted from earth- to ship-fixed points of reference. Fig. 23 presents the safety contour (see Fig. 22 (c)) from the own ship perspective at various observation points. The processed data led to the identification of key grounding risk areas corresponding to forward and side grounding. The grounding avoidance behaviours were identified using the proposed ABGD-M method for the detected 6 shallow waters (see Fig. 22) by comparing the operational characteristics of the main two traffic clusters (see Section 2.2 and Step (ii) of the procedure outlined in Fig. 2). As shown in Fig. 16 the analysis accounted for 2059 voyages from Helsinki to Tallin and 1980 voyages in the opposite direction. The detected potential grounding scenarios were concentrated in several areas, defined as hotspots. The results were summarized in Table 6. Specifically, for side grounding 6 hotspots were identified from Tallin to Helsinki and vice versa. However, for forward grounding hotspots between Helsinki and Tallin where 4 against 6 in the opposite direction (see Figs. 24 (a), (b) and 25 (a), (b)). This is because, for the same shallow water, the grounding situations were diffident among the main two traffic clusters. Forward grounding events from Helsinki to Tallinn in way of hotspots 1 and 3 were not evident. In principle, these results indicate that waterway complexity and grounding risks may be diverse.

3.2.3. Analysis of grounding avoidance behavior

As part of this process, ship grounding avoidance behaviors of potential forward / side grounding scenarios were analyzed for various shallow water areas in various hydro-meteorological conditions. The safety distance to shallow waters along different ship routes was sort listed using (i) a violin plot to represent the probability density distribution of the data at different values, (ii) a box plot in violin plot to indicate the interquartile ranges (Fig. 26 (a)). Notable, for the detected potential forward grounding scenarios from Helsinki to Tallinn hotspots 2 and 4 were used for the analysis of grounding avoidance behaviours. This is because hotspots 1 and 3 contain very few critical scenarios (Fig. 24 (a)).

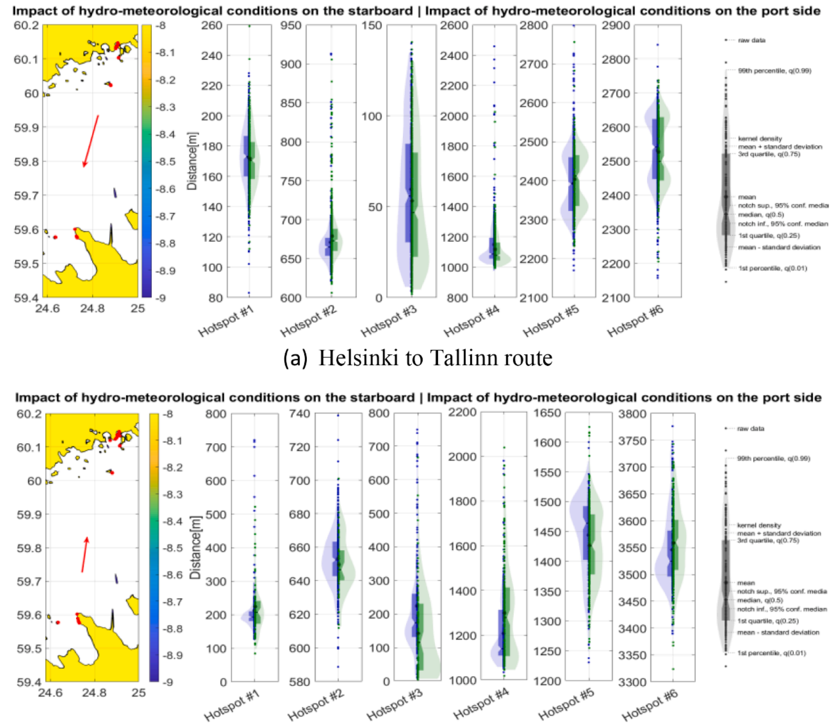

(b) Tallinn to Helsinki route

Fig. 27. Safety distance to shallow waters of side grounding scenarios in various hydro-meteorological conditions (The red points on the map denote the geographical locations of the possible side grounding scenarios due to hydro-meteorological conditions, crew negligence, or technical failure.).

Table 7
Hydro-meteorological parameters cumulative distributions for traffic flow classification.

	Hydro-meteorological condition (cumulative distribution)			
	Calm sea condition		Adverse sea condition	
	<50%		**>50%**	
	25%	**50%**	75%	99%
Wave height(m)	0.219	**0.552**	0.977	2.816
Current speed(m/s)	0.008	**0.0278**	0.061	0.398
Wind speed(m/s)	4.856	**6.741**	8.969	16.323
Swell height(m)	0.111	**0.182**	0.343	1.391

The Gulf of Finland may be ice-covered for several weeks. The ice period (December, January, February) is not considered here as dominating in this area.

To understand the impact of hydro-meteorological conditions, the potential forward grounding scenarios were classified into two groups. The first group included scenarios assuming that the ships sail against the directions of wind and waves and therefore ship bow dynamics dominate sea traffic induced dynamics. The second group assumed that the ships sail along the waves and wind and hence stern ship dynamics are dominant. The distributions of safety distances of two groups were plotted on the two sides of the violin plot. For forward grounding big data analysis led to the following observations:

- Between Helsinki and Tallinn, the distances to avoid grounding ranged between 5500 m and 7500 m with a 98% confidence interval in hotspot 2 and between 5300 and 7300 m with a 98% confidence interval in hotspot 4. In both hotspots the distributions of the distances under the impact of hydro-meteorological conditions on the bow direction were larger (see Fig. 26 (a)).
- Between Tallinn and Helsinki, the distance intervals to avoid grounding varied (see Fig. 26 (b)). For example, the distances to avoid grounding ranged between 1800 m and 4500 m with a 98% confidence interval in hotspot 1 and between 6000 m and 9000 m with a 98% confidence interval in hotspot 4. Similarly, the distributions of the distances under the impact of hydro-meteorological conditions on the bow direction also were larger. For hotspot 3 located in the port the influence of hydro-meteorological conditions may be considered negligible.

On the other hand, the potential side grounding scenarios also were classified into two groups based on the encountered hydro-meteorological conditions, i.e., the directions of the wave, wind, and current in relation to the ship port and starboard [66]. The first group included scenarios assuming that the directions of the wave, wind, and current came from the starboard. The second group assumed that the directions of the wave, wind, and current came from the port of the ship. The results/ findings were summarized as follows:

- Fig. 27 (a) displays side ship grounding avoidance patterns from Helsinki to Tallinn. The distances for the first group to grounding distributions when shallow waters are on the ship starboard are larger than that for the second group (see the locations of hotspots 1, 4, 6 in Fig. 27, and compare the first groups against second groups of hotspots 1, 4,6 in Fig. 22). The opposite seems to be evident when shallow waters are on the port of the ship among the two groups (see the locations of hotspots 2, 3, 5 in Fig. 22 and compare the first groups against second groups of hotspots 2 and 5 in Fig. 27 (a)). The results show that open drift forces become dominant except for hotspot 3 (see hotspot 3 dynamics in the way of port area).
- Fig. 27 (b) presents ship grounding avoidance behaviours from Tallinn to Helsinki. The results indicate that open drift forces under the impact of external environments become dominant to influence the distribution of the safety distances, which are similar to that from Helsinki to Tallinn in Fig. 27(a).

These results indicate that the distances to avoid grounding may be extremely diverse among voyages and hydro-meteorological conditions may impact the ship grounding avoidance behaviour. Understanding the

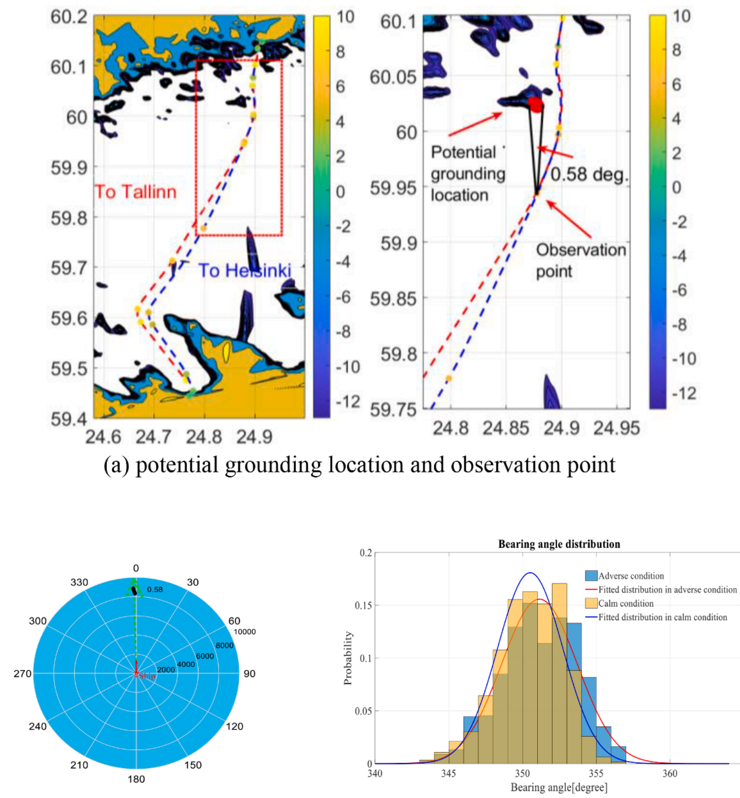

(a) potential grounding location and observation point

(b) ships sail to the shallow waters

(c) bearing angles distribution in adverse sea condition and calm sea condition

Fig. 28. Grounding probabilistic risk evaluation at an observation point from Tallinn to Helsinki.

distance to grounding distribution in safety contours depicted for different routes could improve safety in navigation [68,72].

3.2.4. *Ship grounding probabilistic risk evaluation*

The DP algorithm was used to evaluate ship grounding probabilistic risk. The analysis considered main waypoints of ship routes as observation points (see Fig. 17). Traffic flow scenarios were classified into two groups corresponding to adverse and calm seas (Table 7). Previous research demonstrated that the correlations between ship motion behaviours and swell are low [52]. Hence swell was ignored

Fig. 28 (a) shows the locations of observation points and the distances in between them. Fig. 28 (b) shows that bearing angles were fitted to meet the probabilistic distribution of grounding risk. The bearing angle distribution and the best-fitted distribution (Normal distribution) in both adverse and calm sea conditions are presented in Fig. 28 (c). Shallow waters were located on the port side of the ship route. The critical bearing angles β_1 and β_2 at the observation point towards the shallow waters was estimated to be 359.42° and 0.58°. This indicates that a small number of ships sail in shallow waters (Fig. 28 (b)). The value 0.58° denotes the cumulative bearing angles from the ship to the boundaries of safety contour (see in Fig. 28 (a)).

The geometric probability of grounding P_G at the observation point was estimated as 6.06 $\times 10^{-4}$ in adverse conditions and 2.81 $\times 10^{-5}$ in calm conditions (see Eq. (13) and Fig. 28 (c)). The distance factor k_{DC} was calculated as 2.08 for 4.8 nm distance between the observation point and the boundaries of safety contour (see Eq. (16) and Fig. 28 (a)). The causation probability and risk reduction factors for this navigation area are known from [65] as $P_c = 1.62 \times 10^{-5}$ and $k_{RR} = 0.5$. Based on AIS data records 1980 complete Ro-pax ship trajectories were considered over 2.5 years (see Fig. 16). On this basis the annual grounding frequency was computed as $P_x = 8.09 \times 10^{-6}$ in adverse sea conditions and $P_x = 3.73 \times 10^{-7}$ in calm sea conditions. Differences could be attributed to distinct ship behaviours in different environmental conditions.

Fig. 29 (a) displays that the maximum probability of grounding in adverse and calm sea conditions (see Table 7) for the route from Tallin to Helsinki is 0.04 accidents per year. In the opposite route, this vaue is 0.0138 in adverse conditions and 0.0134 accidents in calm seas. Overall comparisons for various environmental conditions indicates that (i) risks may be diverse (see Fig. 28 versus Fig. 29 (a),(b)) and (ii) the highest value of grounding probabilistic risk from Tallinn to Helsinki is almost 3.07 times more than that of in way of the opposite route. Fig. 30 demonstrates that ship grounding probabilistic risk may be higher before a ship takes an evasive action. In this sense, an observation point can be regarded as a reference warning (see in Section 3.2.1).

To validate the results of grounding probabilistic risk estimates, historical grounding accidents in the Gulf of Finland were reviewed (see Fig. 12). According to casualty reports of FMA, BMEPC and HELCOM over 21 years 10 Ro-Pax ship grounding accidents manifested in 8 waterways (or 16 routes of Ro-Pax ships) [1]. This corresponds to 2.976 $\times 10^{-2}$ accidents / year; a value that is in good agreement with the results predicted (0.04 accidents / year from Tallin to Helsinki and 0.0138 / year in the reverse direction).

3.3. *Uncertainty analysis*

Inaccuracies in data streams, modelling assumptions and method procedures may influence the results. So, the uncertainty analysis (U) should be carried out to quantify the variability of the results due to the variability of inputs. To this end, various uncertainty assessment methods have been proposed [77,78]. In this paper, the commonly applied qualitative approach has been employed, see more applications in [51,69,77]. As shown in Table 8, the uncertainty ratings are defined for uncertainty analysis. Table 9 shows the uncertainty of the various

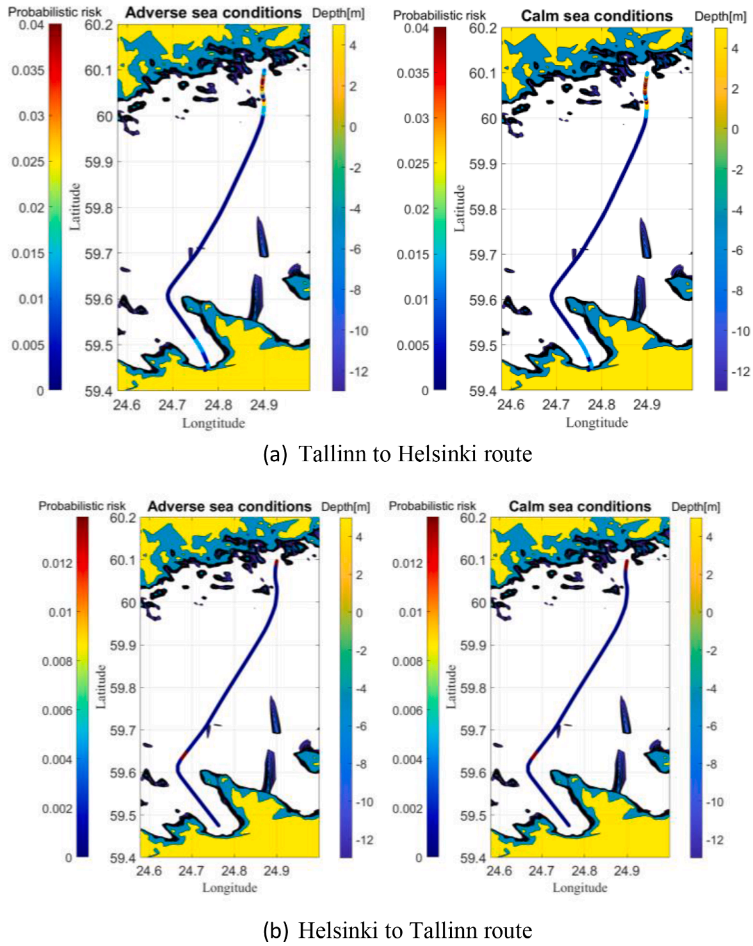

(a) Tallinn to Helsinki route

(b) Helsinki to Tallinn route

Fig. 29. Ship grounding probabilistic risk evaluation along a ship route.

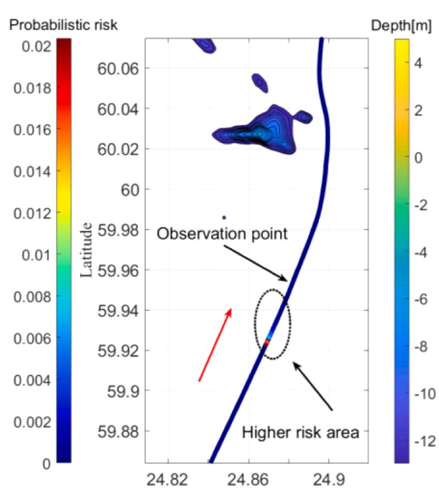

Fig. 30. Ship grounding probabilistic risks before taking evasive action from Tallinn to Helsinki.

factors (data, method, and modelling assumption). It shows that there are generally low uncertainties related to data sources, assumptions, as well as method procedures. Thus, the uncertainties of inputs on the results were judged to be low. On the other hand, the grounding behaviours and probabilistic grounding risks are diverse in various hydro-meteorological conditions and ship voyages, indicating that the hydro-meteorological condition and ship voyages are important influencing risk factors ignored in traditional methods.

Table 8
Interpretation of uncertainty ratings for uncertainty analysis [78].

Aspect	Rating	Interpretation
Uncertainty	L	Many reliable data are available; The phenomena involved are well understood, models are known to give predictions with the required accuracy.
	M	Conditions between those characterizing low and high uncertainty.
	H	Conditions opposite to those characterizing low uncertainty.

In this section, uncertainty analysis is carried out to quantify the probability of grounding as a function of the UKC. The method is tested for a scenario corresponding to the case of a Ro - Pax passenger ship, with a design draft of 7.2 meters that travels from Tallinn to Helsinki (see Figs. 28 (a) and 31(a)). At first, the UKC was set to vary from 10 % to 50 % of the dynamic draft [75,76], and the safety contours corresponding to this variation is shown in Fig. 31 (b). Then, for various safety contours, the grounding probabilities were calculated by following the methodology of Section 3.2.4. Table 10 summarises the variation rates were calculated, indicating that the values of UKC affect the results of the probability of grounding within 5%. The analysis shows that the probabilistic grounding risk has low uncertainty due to the assumption of UKC. This is because the variability of UKC has little effort for the area of shallow waters, see Fig. 31 (b).

Table 9
The uncertainty assessment for grounding avoidance behaviors analysis (U indicates the interpreted rating of uncertainty as outlined in Table 8).

	Model element	U	Justification
Input factors	AIS data	L	Uncertainties may relate to the collection, transmission, and reception of errors [48]. In this case AIS data were reconstructed by trajectory separation, data filtering (i.e., outliers removal), and interpolation over 60 s intervals [1,51] over 2.5 years of shipping operations in the Baltic. Only 4.71% of the used AIS data were filtered and regarded as noising data. This confirms the high quality of data sample [48].
	Bathymetry data	L	GEBCO bathymetry data was used to determine safety contours as explained in Section 2.2. Despite the high accuracy of bathymetry data, it is noted that information on tidal data has not been available for the case study considered.
	Hydro-meteorological data	L	Hydro-meteorological conditions are based on ocean now-cast records from various providers (see Section 3.1). Their accuracy is high as discussed in [48].
Big data analytics models	Ship trajectories clustering method	L	Results demonstrated that different ship trajectories are grouped well into various clusters and therefore the accuracy of this method is rather high (see Section 3.2.1).
	Key waypoints determination	L	A thorough literature survey indicated that the method is efficient enough (see Section 3.2.1 and [2]).
	Ship grounding scenarios detection model	L	A 6-DoF maneuvering Fluid-Structure Interaction (FSI) model [23] was adopted to validate the results of the detected potential grounding scenarios. This approach indicated that 99% of the detected grounding scenarios are linked with unsafe navigation passages [79].
	Probabilistic risk model	L	The probabilistic risk model utilized is based on realistic distributions of ships sailing across unsafe navigation passages [63,64]. The high accuracy of the ship grounding scenarios detection model can also confirm that the probabilistic risk model has low uncertainty.
Assumptions	UKC is 20% of the dynamic draft	L	The literature indicates that UKC always may varyfrom 10 % to 50 % of the dynamic ship draft [59,75,76].The paper assumes that the UKC of large RoPax ships is 20% of the dynamic draft. The values of UKC affect the results of the probability of grounding within 5%, showing that the probabilistic grounding risk has low uncertainty (see Fig. 31 and Table 8).

4. Conclusions

This paper presented a machine learning method for the evaluation of grounding risk in realistic operational conditions. Big data records (AIS, GEBCO, and hydro-meteorological data) of relevance to a Ro-Pax ship operating in the Gulf of Finland over a 2.5-year ice-free period

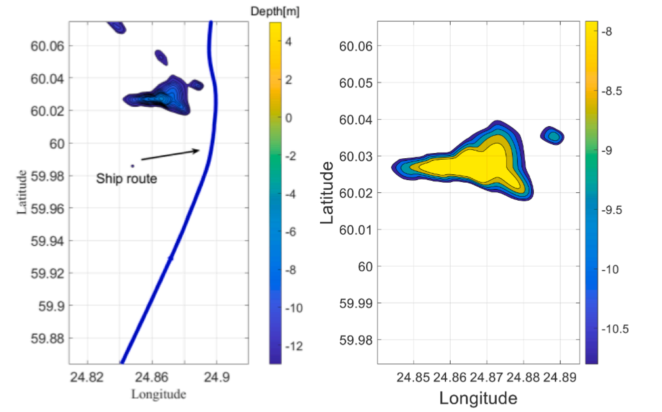

(a) ship route and shallow water (b) safety contours based on various UKC.

Fig. 31. Uncertainty analysis for a potential grounding scenario.

Table 10
The results of uncertainty analysis of the definition of UKC.

UKC	10% × draft	20% × draft (default)	30% × draft	40% × draft	50% × draft
Grounding probability ($\times 10^{-6}$)	8.37	8.46	8.60	8.67	8.85
Variation rate	-0.97%	0	1.67%	2.43%	4.7%

were used to validate this method.

Various forward - and side - grounding scenarios were detected between Tallinn and Helsinki (see Figs. 24 and 25). The analysis of grounding avoidance behaviours has shown that probabilistic risk and timing for triggering grounding avoidance actions may be sensitive to traffic patterns, route, shallow water encounters and environmental conditions (see Fig. 29), which were ignored in traditional methods. The findings may provide important support to the master onboard, as part of an intelligent decision support system for grounding avoidance in real operational conditions. These results are in good agreement with real accident records (see Fig. 12).

It is concluded that big data analytics methods may provide novel insights into grounding risk evaluation and in turn may lead to better evaluation of waterway complexity indices and critical operational scenarios not currently accounted for by existing accident databases. Additionally, they may also provide inputs for the ship motion simulations and design of experiments for use in ship functional safety management. Future work could focus on the use of visual data mining techniques with the aim to understand the influence of ship type, size, visibility etc. on ship traffic behaviour and probability of grounding risk.

CRediT authorship contribution statement

Mingyang Zhang: Writing – original draft, Methodology, Investigation, Formal analysis. **Pentti Kujala:** Writing – review & editing, Resources. **Spyros Hirdaris:** Writing – review & editing, Supervision, Project administration, Methodology, Funding acquisition, Conceptualization.

Declaration of Competing Interest

The authors declare that they have no known competing financial interests or personal relationships that could have appeared to influence the work reported in this paper.

Data Availability

The data that has been used is confidential.

Acknowledgments

The research presented in this paper has received funding from the European Union Project Flooding Accident Response (FLARE) number 814753, under the H2020 program. The authors express their gratitude for this support. The views set out in this paper are those of the authors and do not necessarily reflect the views of their respective organizations.

References

[1] Zhang M, Montewka J, Manderbacka T, Kujala P, Hirdaris S. A big data analytics method for the evaluation of ship-ship collision risk reflecting hydro-meteorological conditions. Reliab Eng Syst Saf 2021;213:107674.
[2] Du L, Banda OAV, Huang Y, Goerlandt F, Kujala P, Zhang W. An empirical ship domain based on evasive maneuver and perceived collision risk. Reliab Eng Syst Saf 2021;213:107752.
[3] Zhang W, Goerlandt F, Kujala P, Wang Y. An advanced method for detecting possible near miss ship collisions from AIS data. Ocean Eng 2016;124:141–56.
[4] Carter T, Williams JG, Roberts SE. Crew and passenger deaths from vessel accidents in United Kingdom passenger ships since 1900. Int Marit Health 2019;70(1):1–10.
[5] Zhang M, Montewka J, Manderbacka T, Kujala P, Hirdaris S. Analysis of the grounding avoidance behavior of a Ro-Pax ship in the Gulf of Finland using big data. In: Proceedings of the 30th international ocean and polar engineering conference; 2020.
[6] MAIB. Maritime Casualties reported to UK Marine Accident Investigation Branch from 2005 –2018 (includes non-tidal waters and rivers). Marine Accident Investigation Branch 2018. Retrieved on 13.06.22 from: http://marine.gov.scot/maps/403.
[7] Zhang M, Conti F, Le Sourne H, Vassalos D, Kujala P, Lindroth D, Hirdaris S. A method for the direct assessment of ship collision damage and flooding risk in real conditions. Ocean Eng 2021;237:109605.
[8] Yu Q, Teixeira ÂP, Liu K, Rong H, Soares CG. An integrated dynamic ship risk model based on Bayesian networks and evidential reasoning. Reliab Eng Syst Saf 2021;216:107993.
[9] HELCOM. Report on shipping accidents in the Baltic Sea from 2014 to 2017. Baltic Marine Environment Protection Commission 2018. Retrieved on 21.03.22 from: https://helcom.fi/baltic-sea-trends/maritime/accidents/.
[10] Pedersen PT. Collision and grounding mechanics. Proc WEMT 1995;95(1995):125–57.
[11] Zhang Y, Sun X, Chen J, Cheng C. Spatial patterns and characteristics of global maritime accidents. Reliab Eng Syst Saf 2021;206:107310.
[12] Youssef SAM, Paik JK. Hazard identification and scenario selection of ship grounding accidents. Ocean Eng 2018;153:242–55.
[13] Gucma L. The method of navigational risk assessment on waterways based on generalised real time simulation data. In: Proceedings of the international conference on marine simulation and ship maneuverability; 2006.
[14] Sakar C, Toz AC, Buber M, Koseoglu B. Risk analysis of grounding accidents by mapping a fault tree into a Bayesian network. Appl Ocean Res 2021;113:102764.
[15] Senol YE, Aydogdu YV, Sahin B, Kilic I. Fault tree analysis of chemical cargo contamination by using fuzzy approach. Expert Syst Appl 2015;42(12):5232–44.
[16] Montewka J, Hinz T, Kujala P, Matusiak J. Probability modelling of vessel collisions. Reliab Eng Syst Saf 2010;95(5):573–89.
[17] Akhtar MJ, Utne IB. Human fatigue's effect on the risk of maritime groundings–a Bayesian network modeling approach. Saf Sci 2014;62:427–40.
[18] Montewka J, Krata P, Goerlandt F, Mazaheri A, Kujala P. Marine traffic risk modelling–an innovative approach and a case study. Proc Inst Mech Eng Part O J Risk Reliab 2011;225(3):307–22.
[19] Abaei MM, Arzaghi E, Abbassi R, Garaniya V, Javanmardi M, Chai S. Dynamic reliability assessment of ship grounding using Bayesian inference. Ocean Eng 2018;159:47–55.
[20] Hänninen M, Kujala P. Bayesian network modeling of port state control inspection findings and ship accident involvement. Expert Syst Appl 2014;41(4):1632–46.
[21] Yu Q, Liu K, Yang Z, Wang H, Yang Z. Geometrical risk evaluation of the collisions between ships and offshore installations using rule-based Bayesian reasoning. Reliab Eng Syst Saf 2021;210:107474.
[22] Tabri K, Naar H, Kõrgesaar M. Ultimate strength of ship hull girder with grounding damage. Ships Offshore Struct 2020;15(sup1):S161–75.
[23] Taimuri G, Kim SJ, Mikkola T, Hirdaris S. A Two-way coupled FSI model for the rapid evaluation of accidental loads following ship hard grounding events. J Fluids Struct 2022;112:103589.
[24] Kim SJ, Korgersaar M, Ahmadi N, Taimuri G, Kujala P, Hirdaris S. The influence of fluid structure interaction modelling on the dynamic response of ships subject to collision and grounding. Mar Struct 2021;75:102875.
[25] Pineau JP, Le Sourne H, Soulhi Z. Rapid assessment of ship raking grounding on elliptic paraboloid shaped rock. Ships Offshore Struct 2021;16(sup1):106–21.
[26] Bulian G, Cardinale M, Dafermos G, Lindroth D, Ruponen P, Zaraphonitis G. Probabilistic assessment of damaged survivability of passenger ships in case of grounding or contact. Ocean Eng 2020;218:107396.
[27] Bužančić Primorac B, Parunov J, Guedes Soares C. Structural reliability analysis of ship hulls accounting for collision or grounding damage. J Mar Sci Appl 2020;19(4):717–33.
[28] Bergström M, Erikstad SO, Ehlers S. Assessment of the applicability of goal-and risk-based design on Arctic sea transport systems. Ocean Eng 2016;128:183–98.
[29] Szlapczynska J, Szlapczynski R. Preference-based evolutionary multi-objective optimization in ship weather routing. Appl Soft Comput 2019;84:105742.
[30] Wibisono E, Jittamai P. Multi-objective evolutionary algorithm for a ship routing problem in maritime logistics collaboration. Int J Logist Syst Manag 2017;28(2):225–52.
[31] Xie L, Xue S, Zhang J, Zhang M, Tian W, Haugen S. A path planning approach based on multi-direction A* algorithm for ships navigating within wind farm waters. Ocean Eng 2019;184:311–22.
[32] Zhang C, Zhang D, Zhang M, Mao W. Data-driven ship energy efficiency analysis and optimization model for route planning in ice-covered Arctic waters. Ocean Eng 2019;186:106071.
[33] Liang C, Zhang X, Han X. Route planning and track keeping control for ships based on the leader-vertex ant colony and nonlinear feedback algorithms. Appl Ocean Res 2020;101:102239.
[34] Mohan BC, Baskaran R. A survey: ant colony optimization based recent research and implementation on several engineering domain. Expert Syst Appl 2012;39(4):4618–27.
[35] Yan XP, Wang SW, Ma F, Liu YC, Wang J. A novel path planning approach for smart cargo ships based on anisotropic fast marching. Expert Syst Appl 2020;159:113558.
[36] Chen P, Huang Y, Papadimitriou E, Mou J, van Gelder P. Global path planning for autonomous ship: a hybrid approach of fast marching square and velocity obstacles methods. Ocean Eng 2020;214:107793.
[37] Gil M. A concept of critical safety area applicable for an obstacle-avoidance process for manned and autonomous ships. Reliab Eng Syst Saf 2021;214:107806.
[38] Gil M, Montewka J, Krata P, Hinz T, Hirdaris S. Semi-dynamic ship domain in the encounter situation of two vessels. Developments in the collision and grounding of ships and offshore structures. Boca Raton, FL, USA: CRC Press; 2019. p. 301–7.
[39] Gil M, Montewka J, Krata P, Hinz T, Hirdaris S. Determination of the dynamic critical maneuvering area in an encounter between two vessels: operation with negligible environmental disruption. Ocean Eng 2020;213:107709.
[40] Montewka J, Manderbacka T, Ruponen P, Tompuri M, Gil M, Hirdaris S. Accident susceptibility index for a passenger ship-a framework and case study. Reliab Eng Syst Saf 2022;218:108145.
[41] Cao J, Liang M, Li Y, Chen J, Li H, Liu RW, Liu J. PCA-based hierarchical clustering of AIS trajectories with automatic extraction of clusters. In: Proceedings of the IEEE 3rd international conference on big data analysis (ICBDA). IEEE; 2018. p. 448–52.
[42] Xin X, Liu K, Yang Z, Zhang J, Wu X. A probabilistic risk approach for the collision detection of multi-ships under spatiotemporal movement uncertainty. Reliab Eng Syst Saf 2021;215:107772.
[43] Li H, Liu J, Wu K, Yang Z, Liu RW, Xiong N. Spatio-temporal vessel trajectory clustering based on data mapping and density. IEEE Access 2018;6:58939–54.
[44] Kokkinakos P, Michalitsi-Psarrou A, Mouzakitis S, Alvertis I, Askounis D, Koussouris S. Big data exploitation for maritime applications a multi-segment platform to enable maritime big data scenarios. In: Proceedings of the international conference on engineering, technology and innovation (ICE/ITMC). IEEE; 2017. p. 1131–6.
[45] Li L, Lu W, Niu J, Liu J, Liu D. AIS data-based decision model for navigation risk in sea areas. J Navig 2018;71(3):664–78.
[46] Xue J, Wu C, Chen Z, Van Gelder PHAJM, Yan X. Modeling human-like decision-making for inbound smart ships based on fuzzy decision trees. Expert Syst Appl 2019;115:172–88.
[47] Chai T, Weng J, De-qi X. Development of a quantitative risk assessment model for ship collisions in fairways. Saf Sci 2017;91:71–83.
[48] Hirdaris, S., Zhang, M., Montewka, J., and Manderbacka, T. Analysis of routing and traffic data. EU Project on FLooding Accident REsponse (FLARE), Work Package WP2, Deliverable Report D2.4, 2020. (Retrieved on 13.06.22 from: https://flare-project.eu/images/downloads/191028_FLARE_Deliverable_2.2_Final.pdf).
[49] Tu E, Zhang G, Rachmawati L, Rajabally E, Huang GB. Exploiting AIS data for intelligent maritime navigation: a comprehensive survey from data to methodology. IEEE Trans Intell Transp Syst 2017;19(5):1559–82.
[50] Xin X, Liu K, Yang X, Yuan Z, Zhang J. A simulation model for ship navigation in the "Xiazhimen" waterway based on statistical analysis of AIS data. Ocean Eng 2019;180:279–89.
[51] Zhang M, Zhang D, Fu S, Kujala P, Hirdaris S. A predictive analytics method for maritime traffic flow complexity estimation in inland waterways. Reliab Eng Syst Saf 2022:108317.
[52] Zhang M, Kujala P, Musharraf M, Matuisiak J, Zhang J, Hirdaris S. A machine learning method for the prediction of ship motion trajectories in real operational conditions. Saf Sci (Forthcom) 2022.
[53] Zhang S, Shi G, Liu Z, Zhao Z, Wu L. Data-driven based automatic maritime routing from massive AIS trajectories in the face of disparity. Ocean Eng 2018;155:240–50.
[54] Yuan X, Zhang D, Zhang J, Zhang M, Soares CG. A novel real-time collision risk awareness method based on velocity obstacle considering uncertainties in ship dynamics. Ocean Eng 2021;220:108436.
[55] Wei Z, Xie X, Zhang X. AIS trajectory simplification algorithm considering ship behaviours. Ocean Eng 2020;216:108086.
[56] Du L, Goerlandt F, Banda OAV, Huang Y, Wen Y, Kujala P. Improving stand-on ship's situational awareness by estimating the intention of the give-way ship. Ocean Eng 2020;201:107110.
[57] Wessel P, Luis JF, Uieda L, Scharroo R, Wobbe F, Smith WHF, Tian D. The generic mapping tools version 6. Geochem Geophys Geosyst 2019;20(11):5556–64.
[58] Bagnardi M, González PJ, Hooper A. High-resolution digital elevation model from tri-stereo Pleiades-1 satellite imagery for lava flow volume estimates at Fogo Volcano. Geophys Res Lett 2016;43(12):6267–75.

[59] Verwilligen J, Eloot K, Mansuy M, Vantorre M. Full-scale measurements of vertical motions on ultra large container vessels in Scheldt estuary. Ocean Eng 2019;188: 106264.

[60] Goerlandt F, Montewka J, Zhang W, Kujala P. An analysis of ship escort and convoy operations in ice conditions. Saf Sci 2017;95:198–209.

[61] Liu RW, Nie J, Garg S, Xiong Z, Zhang Y, Hossain MS. Data-driven trajectory quality improvement for promoting intelligent vessel traffic services in 6G-enabled maritime IoT systems. IEEE Internet Things J 2020;8(7):5374–85.

[62] Liu RW, Yuan W, Chen X, Lu Y. An enhanced CNN-enabled learning method for promoting ship detection in maritime surveillance system. Ocean Eng 2021;235: 109435.

[63] COWI. Risk analysis for sea traffic in the area around Bornholm. Tech. Rep. 2008 P-65775–002Danish Maritime Authority.

[64] Liu Y, Frangopol DM. Probabilistic risk, sustainability, and utility associated with ship grounding hazard. Ocean Eng 2018;154:311–21.

[65] Mazaheri A, Montewka J, Kujala P. Towards an evidence-based probabilistic risk model for ship-grounding accidents. Saf Sci 2016;86:195–210.

[66] Zhou Y, Daamen W, Vellinga T, Hoogendoorn SP. Ship classification based on ship behavior clustering from AIS data. Ocean Eng 2019;175:176–87.

[67] Yang D, Wu L, Wang S, Jia H, Li KX. How big data enriches maritime research–a critical review of automatic identification system (AIS) data applications. Transp Rev 2019;39(6):755–73.

[68] Zhang M, Zhang D, Fu S, Yan X, Goncharov V. Safety distance modeling for ship escort operations in Arctic ice-covered waters. Ocean Eng 2017;146:202–16.

[69] Zhang M, Zhang D, Goerlandt F, Yan X, Kujala P. Use of HFACS and fault tree model for collision risk factors analysis of icebreaker assistance in ice-covered waters. Saf Sci 2019;111:128–43.

[70] Zhang W, Feng X, Qi Y, Shu F, Zhang Y, Wang Y. Towards a model of regional vessel near-miss collision risk assessment for open waters based on AIS data. J Navig 2019;72(6):1449–68.

[71] Liang M, Zhan Y, Liu RW. MVFFNet: multi-view feature fusion network for imbalanced ship classification. Pattern Recognit Lett 2021;151:26–32.

[72] Gil M, Kozioł P, Wróbel K, Montewka J. Know your safety indicator–a determination of merchant vessels bow crossing range based on big data analytics. Reliab Eng Syst Saf 2022;220:108311.

[73] Rong H, Teixeira AP, Soares CG. Spatial correlation analysis of near ship collision hotspots with local maritime traffic characteristics. Reliab Eng Syst Saf 2021;209: 107463.

[74] Rong H, Teixeira AP, Soares CG. Maritime traffic probabilistic prediction based on ship motion pattern extraction. Reliab Eng Syst Saf 2022;217:108061.

[75] Scully B, Young D. Evaluating the underkeel clearance of historic vessel transits in the southwest pass of the Mississippi river. J Waterw Port Coast Ocean Eng 2021; 147(5):05021008.

[76] Orseau S, Huybrechts N, Tassi P, Kaidi S, Klein F. NavTEL: open-source decision support tool for ship routing and underkeel clearance management in estuarine channels. J Waterw Port Coast Ocean Eng 2021;147(2):04020053.

[77] Flage R, Aven T. Expressing and communicating uncertainty in relation to quantitative risk analysis. Reliability: Theory & Applications 2009;(4.2-1(13)): 9–18.

[78] Goerlandt F, Reniers G. On the assessment of uncertainty in risk diagrams. Saf Sci 2016;84:67–77.

[79] Taimuri G, Zhang M, Hirdaris S. A predictive method for the avoidance of ship grounding in real operational conditions. In: Proceedings of the SNAME maritime convention OnePetro; 2022.